Location of Magnetic and Fluorescent Nanoparticles Encapsulated inside Giant Liposomes

Grégory Beaune, Christine Ménager,* and Valérie Cabuil

UPMC Univ Paris 06/CNRS/ESPCI/UMR 7612, Laboratoire Liquides Ioniques et Interfaces Chargées, case courrier 63, 4 place Jussieu, 75252 Paris Cedex 05, France

Received: December 17, 2007; Revised Manuscript Received: April 4, 2008

In this paper, we demonstrate the production of highly magnetic and fluorescent giant vesicles by encapsulating γ-Fe_2O_3−rhodamine B nanoparticles. The liposomes containing the nanoparticles were made of 1,2-dioleoyl-*sn*-glycero-3-phosphocholine (DOPC). We found that the ionic strength of the initial magnetic fluid is a crucial parameter in controlling the physicochemical properties of the bilayer. At high ionic strength, we obtained very important deformations of liposomes with high magnetic susceptibilities induced by an applied magnetic field. The encapsulation rate was studied using magnetophoresis and photobleaching tests, and the membrane properties were studied using confocal microscopy and elastic measurements.

Introduction

Liposomes are promising drug carriers because they can encapsulate hydrophobic compounds within their bilayers[1,2] as well as hydrophilic substances within their internal aqueous compartments.[3] According to their size, liposomes are used either as cellular models (in the case of giant unilamellar vesicles, so-called GUVs) or for in vivo applications (in the case of large unilamellar vesicles (LUVs) with a diameter <1 μm). Liposomes are easy to synthesize, biocompatible, and nontoxic and can be made magnetic by encapsulating magnetic nanoparticles or fluorescent by grafting an organic dye onto a lipid of the membrane[11] or by encapsulating quantum dots.[12] Magnetic LUVs are used in biomedical applications as agents to control drug release,[7] contrast agents in magnetic resonance imaging (MRI),[8,9] or as agents for hyperthermia.[10] Magnetic GUVs are used as cellular models to test the membrane properties from their deformation in a magnetic field,[4] or to study pore formations.[5,6] Locating a fluorescence dye in the aqueous core of the liposome allows one to measure membrane permeability[14] and to more easily visualize liposome deformations.[15]

Although the literature includes reports on magnetic or fluorescent GUVs or LUVs, little has been reported on the association between these properties. Fluorescent antibodies have been grafted onto magnetoliposomes and internalized inside cells for visualization and cell sorting by magnetic separation.[16] Encapsulation of magnetic nanoparticles and quantum dots in the same liposomes has also been described in a proposed multifunctional system for both MRI and fluorescence microscopy.[17,18] It appears that the location of both types of nanoparticles inside these objects is strongly related to the procedure used in their synthesis. Both the hydrophilic property of magnetic nanoparticles and the lipophilic property of quantum dots complicate the interpretation of observations because each type of particle can localize and behave differently. Here, we describe the process of encapsulation in the GUV of nanoparticles that are by themselves magnetic and fluorescent, i.e., rhodamine-grafted maghemite nanoparticles.[19] The main advantage of these bifunctional particles is that confocal microscopy can be used to locate the particles inside the liposomes. This allows one to study the relationship between the deformation of liposomes when a magnetic field is applied and the location of the particles.

Experimental Section

Materials. The *cis*-1,2-dioleoyl-*sn*-glycero-3-phosphocholine (DOPC), dimercaptosuccinic acid (DMSA), rhodamine B, 1-ethyl-3-(3-dimethylaminopropyl)-carbodiimide (EDC), and cystamine used were all purchased from Sigma-Aldrich.

Synthesis of Maghemite Nanoparticles. Using a procedure that has been described previously,[20] superparamagnetic magnetite Fe_3O_4 nanocrystals were prepared from an alkaline coprecipitation of $FeCl_2$ and $FeCl_3$, in which 180 g of the Fe^{II} salt (0.9 mol) and 715 mL of the Fe^{III} solution (1.5 mol) were mixed in an acidic medium (HCl). Magnetite (Fe_3O_4) particles were coprecipitated by rapid addition of a concentrated ammonia solution (20%, 1 L). After acidification with a nitric acid solution (360 mL, 2 mol L^{-1}), the addition of 800 mL of a boiling solution of ferric nitrate (323 g, 1.3 mol) led to the chemical oxidation of magnetite to maghemite.

The resulting nanoparticles were composed of monocrystalline ferrimagnetic monodomains of maghemite with a crystallite diameter around 8 nm and a positive surface charge. These were dispersed in water, leading to a stable aqueous colloidal dispersion with pH 1−3, according to the degree of dilution (acidic ferrofluid).

Synthesis of an Aqueous Dispersion of Citrate-Coated Maghemite Nanoparticles (Cit-FF). The maghemite particles were decanted and sieved, and then heated to 80 °C for 30 min in water supplemented with 70 g of sodium citrate, precipitated in acetone at 25 °C, and then filtered. Final adjustment of both the aqueous medium and the maghemite concentration was achieved by ultrafiltration (MACROSEP filter, cutoff = 50 kDa, Fisher Scientific Labosi, France).

Synthesis of Rhodamine B Magnetic Fluid (Rh-FF). The process used has been described previously,[20] and is based on the complexation of DMSA molecules on positively charged γ-Fe_2O_3 particles. The DMSA is coupled to the particles by at least one carboxyl and one thiol group. Ungrafted thiol groups are available for subsequent coupling, and any unadsorbed carboxylate groups ensure a surface charge is present. The molar ratios for the process were 10% DMSA/Fe and 25% dye/DMSA, and these ratios correspond to the maximum rate of coupling.

* Corresponding author. E-mail: christine.menager@upmc.fr.

10.1021/jp711811u CCC: $40.75
Published on Web 05/31/2008

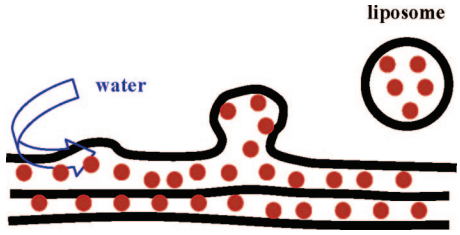

Figure 1. Preparation of magnetoliposomes using a spontaneous swelling process.

A total of 320 mg of rhodamine B, 149 mg of EDC, and 90 mg of cystamine were stirred in 500 mL of water for a period of 3 h at pH 7. Then, 500 mg of DMSA and 8.4 mL of an acidic ferrofluid ([Fe] = 3 mol L^{-1}, pH 1.17) were added, and the mixture was stirred for 2 h. Flocculation occurred, and the flocculate was separated rapidly from the supernatant using a permanent magnet. This was then washed twice with water. Then, 500 mL of water was added, the pH was increased to pH 9 by adding tetramethylammonium hydroxide (TMAOH) (1 mol L^{-1}), and the magnetic material was stirred in this alkaline medium for 45 min. This step allowed the magnetic particles to redisperse in water. The pH was adjusted to pH 7 using 1 mol L^{-1} HCl.

Finally, the particles were submitted to successive precipitation to eliminate any nonadsorbed rhodamine. NaCl was added to the solution until the ferrofluid was destabilized (~0.1 g of NaCl powder for 10 mL of magnetic fluid). At this time, the liquid became turbid, and the precipitation of the particles was accelerated under a magnetic field gradient using a strong NdFeB magnet. Magnetic separation continued stepwise until the supernatant was colorless.

Control of the Ionic Strength and Concentration of the Magnetic Fluids. Ultrafiltration was used to concentrate the particles in the magnetic fluids. In the case of rhodamine-coated particles, a 10 mL aliquot of the Rh-FF suspension was centrifuged in a MACROSEP filter (cutoff = 30 kD, Fisher Scientific Labosi) at 5000 rpm for 30 min. The ionic strength was measured from the conductivity. The properties of Rh-FF were as follows: σ = 540 μS and [Fe] = 6.6 mol L^{-1}. The same process was used for the citrate-coated particles, and the properties of the magnetic fluid obtained were σ = 576 μS and [Fe] = 6.6 mol L^{-1}.

Synthesis of the Magnetic and Fluorescent Liposomes. The preparation of magnetoliposomes has been described elsewhere.[4] Encapsulation of a magnetic fluid inside liposomes was performed using a spontaneous swelling procedure. The first step was to prehydrate the phospholipid film with a colloidal solution of nanoparticles, and the second step was to swell it with pure water (Figure 1).

The ionic strength of the solution encapsulated inside liposomes was adjusted before encapsulation by adding NaCl. Sodium chloride (16 or 28 mg) was mixed with the magnetic fluid (100 μL) to obtain [NaCl] = 2.74 mol L^{-1} or [NaCl] = 4.79 mol L^{-1} in the magnetic fluid. A small mass of perfectly dry DOPC powder (around 1 mg) was placed in a glass Petri dish. A total of 10 μL of the γ-Fe_2O_3/NaCl mixture was added, and the mixture was spread and sheared with a glove finger to obtain a fat and oily orange film. This film was presumably a lamellar phase swelled with charged particles. Immediately following the shearing, 1.5 mL of distilled water was poured onto the fatty film to start the spontaneous swelling of the liposomes. The samples were placed in a water bath at 45 °C and observed after 30 min using an optical microscope.

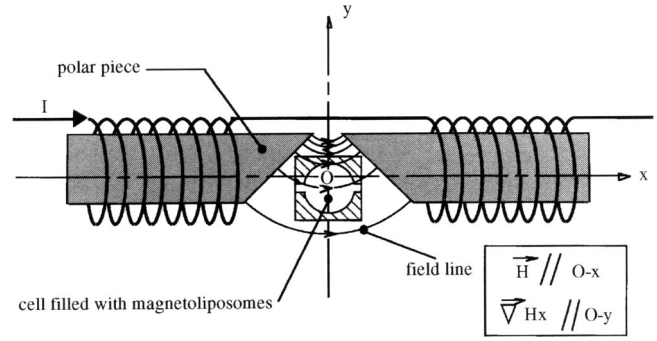

Figure 2. The magnetophoresis experimental setup. The sample containing the magnetoliposomes was placed between the two coils in a capillary tube.

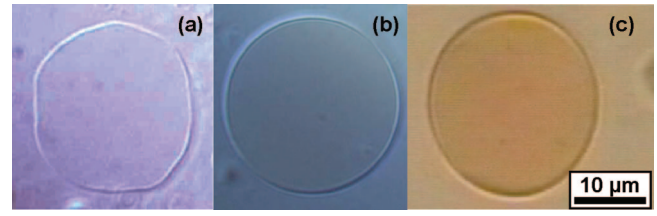

Figure 3. Optical microscopic images of liposomes encapsulating Rh-FF: (a) without NaCl, Nomarsky contrast (DIC), (b) with [NaCl] = 2.74 mol L^{-1} (Nomarsky contrast (DIC)), and (c) with [NaCl] = 4.79 mol L^{-1}.

Optical Microscopy. The samples were imaged using transmitted light and epifluorescence microscopy using an inverted microscope (Leica 40×, numerical aperture (NA) = 0.65) equipped with a 100 W mercury lamp. A fluorescence filter cube with a 546 nm excitation filter (BP546/10) and a 590 nm emission filter (LP 590) was used to visualize rhodamine B fluorescence. Pictures from a charge-coupled-device camera were digitized with a frame grabber (LG-3, Scion Corp., Frederick, MD).

Confocal laser scanning microscopy was performed using a Leica TCS SP2 confocal laser scanning microscope equipped with a 40× oil immersion objective with NA = 1.25 and a 63× oil immersion objective with NA = 1.40. Rhodamine B was excited with the 543 nm line of a He−Ne laser with an excitation power of 75 mW, and was detected at a wavelength of 729 nm (red). Images (512 × 512 pixels, resolution = 183 nm, scan speed = 400 Hz) were exported from the instrument software in JPG format and visualized using the Image J software package v. 1.35s (National Institutes of Health, Bethesda, MD).

Magnetophoresis Measurements. The migration of the magnetoliposomes under a controlled magnetic field gradient was used to estimate the magnetic load after determining the liposome mean velocity. Briefly, the magnetophoresis assay involved following the movement of magnetically labeled liposomes using a magnetic field gradient perpendicular to the applied magnetic field. The field lines of two coils in series were deviated by polar pieces with a 45° edge, with the sample situated in the middle region, as shown in Figure 2. The gradient was 65 ± 2 Oe cm^{-1} (measured with Hall probes) with the field equal to 150 ± 2 Oe in the sample place.

The magnetic force experienced by each liposome had a constant value of

$$F_m = \mu_0 \chi H_y (\nabla_x H_y) V \quad (1)$$

where μ_0 is the permeability of a vacuum, H_y is the applied magnetic force, $\nabla_x H_y$ is the magnetic field gradient, V is the volume of the liposome, and η is the magnetic susceptibility.

TABLE 1: Summary of the Mean Values of χ and φ Obtained with Different NaCl Concentrations Using Cit-FF and Rh-FF

		[NaCl] 0 mol L^{-1}	[NaCl] 2.74 mol L^{-1}	[NaCl] 4.79 mol L^{-1}
Rh-FF liposomes	χ	5.5×10^{-3}	3.1×10^{-3}	2.1×10^{-2}
	φ (%)	3.7×10^{-2}	2.1×10^{-2}	0.14
	number of liposomes	13	12	11
Cit-FF liposomes	χ	2.1×10^{-3}	3.2×10^{-3}	2.4×10^{-2}
	φ (%)	2.0×10^{-2}	3.1×10^{-2}	0.25
	number of liposomes	17	12	19

In the approximation of a weak magnetic field (i.e., for spherical liposomes), the viscous force is $F_v = 6\pi\eta R v$. When the permanent regime was reached, the magnetic force was exactly balanced by the viscous force

$$F_m = F_v = 6\pi\eta R v \quad (2)$$

where η is the viscosity of water, R is the liposome radius, and v is the liposome velocity. Thus, the magnetic susceptibility can be obtained using the following expression

$$\chi_{ves} = \frac{9\eta v}{2\mu_0 H_y (\nabla_x H_y) R^2} \quad (3)$$

The volume fraction of particles in the vesicles (φ_{ves}) can be obtained knowing the initial magnetic fluid properties

$$\varphi_{ves} = \chi_{ves}\left(\frac{\varphi_{FF}}{\chi_{FF}}\right) \quad (4)$$

where φ_{FF} is the volume fraction of particles in the magnetic fluid and χ_{FF} is the magnetic susceptibility of the magnetic fluid.

Results

Effect of the Ionic Strength on the Encapsulation Efficiency. Magnetic and fluorescent liposomes encapsulating Rh-FF and magnetic liposomes encapsulating Cit-FF were synthesized without adding any salt (test sample), or by adding NaCl at one of two concentrations ([NaCl] = 2.74 or 4.79 mol L^{-1}), as described in the Experimental Section. Increasing the concentration of salt increased the viscosity of the liquid in the case of Rh-FF encapsulation. Figure 3 shows optical microscopic images of three samples.

Qualitatively, the contrast between the inside of the liposomes and their surrounding environment increased with increasing salt concentration of the encapsulated magnetic fluid. In the case of liposomes encapsulating Rh-FF, the color of the liposomes changed from a pale to a steady brown, characteristic of the color of the magnetic fluids, as the salt concentration increased. We noticed the absence of membrane fluctuation when the liposomes were obtained with a high concentration of salt. In addition, the membrane appeared very thick and contrasting in this case.

The increase in the volume fraction of the nanoparticles encapsulated inside the fluorescent and magnetic liposomes with increasing concentration of salt was confirmed from the magnetophoresis data. Table 1 summarizes the mean values of χ and φ for each type of liposome. The standard deviation is important (see the Supporting Information), because a swelling process was used to prepare the magnetoliposomes.

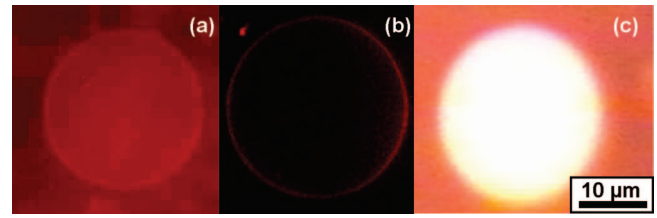

Figure 4. Fluorescent optical microscopic images of liposomes encapsulating Rh-FF: (a) [NaCl] = 0 mol L^{-1} (exposure time = 15 s, contrast = 50, brightness = 0, gamma = 1.50), (b) [NaCl] = 2.74 mol L^{-1} (exposure time = 2 s, contrast = 30, brightness = 0, gamma = 1.50), and (c) [NaCl] = 4.79 mol L^{-1} (exposure time = 66 ms, contrast = 0, brightness = 0, gamma = 1.50).

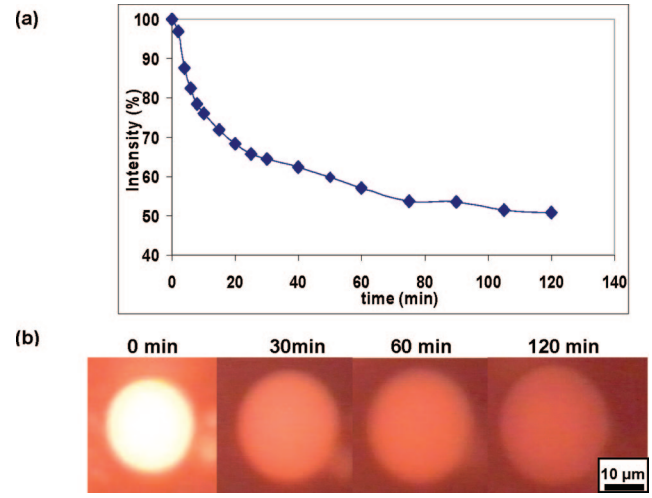

Figure 5. Photobleaching test (using a 100 W Hg lamp): (a) temporal evolution of the fluorescence intensity for liposomes encapsulating Rh-FF synthesized with [NaCl] = 4.79 mol L^{-1} and (b) fluorescence images of the liposome studied in part a (exposure time = 66 ms, contrast = 0, brightness = 0, gamma = 1.50).

The encapsulation efficiency increased by a factor of 100 when the concentration of salt added increased from 0 to 4.79 mol L^{-1}.

Effect of the Added Salt on the Fluorescence Properties. Fluorescence optical microscopy of the liposomes showed that higher salt concentrations increased the fluorescence intensity because of the increase in volume fraction of the magnetic particles (Figure 4).

This fluorescence intensity of liposomes obtained with a high salt concentration allowed us to perform a photobleaching test, in which the decrease in the fluorescence intensity of the liposome was studied as a function of time (Figure 5).

This test showed that the fluorescence of the liposome was visible for 2 h, despite the presence of an organic dye. These good fluorescent properties can be used to perform long-term visualization experiments. This experiment also showed that fluorescence is important, despite the quenching caused by the interaction between maghemite particles and rhodamine.

At the highest concentration of salt, the fluorescence appeared to be homogeneous over the entire volume of the liposome, and when no salt was added, even when the fluorescence covered the entire volume of the liposome, it seemed much more intense at the level of the membrane. Confocal microscopy was performed to localize the fluorescence (Figure 6).

The confocal cross-sectional images in Figure 6 confirm that the fluorescence was much more intense at the membrane level either with or without a moderate salt concentration. Note that, in Figure 6a, the picture has been adjusted so that the back of

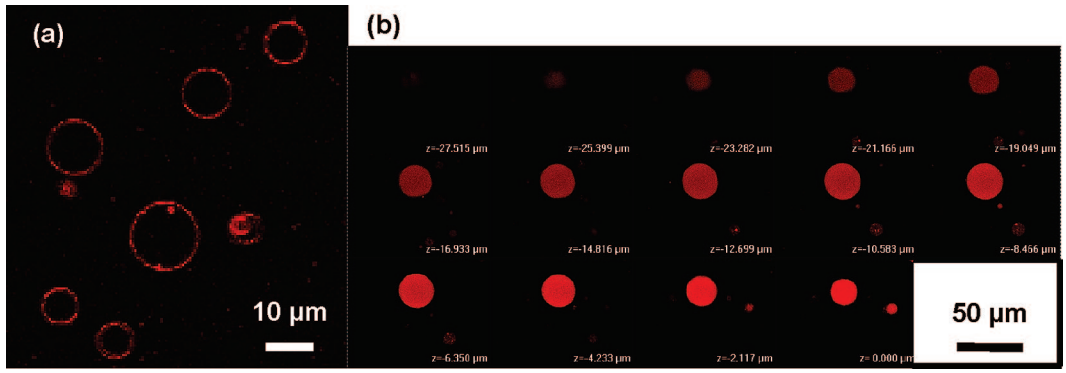

Figure 6. Confocal cross-sectional images of fluorescent magnetoliposomes: (a) [NaCl] = 2.74 mol L^{-1} (pinhole = 115 μm) and (b) different cross sections of a magnetic and fluorescent liposome with [NaCl] = 4.79 mol L^{-1} (pinhole 81 μm).

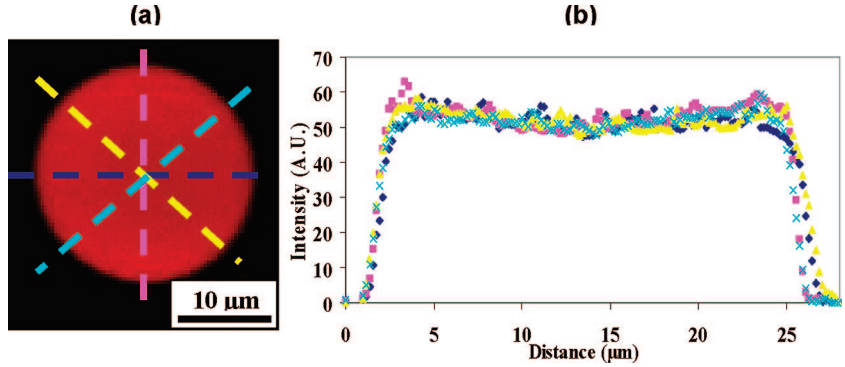

Figure 7. (a) Confocal cross-sectional image of a liposome encapsulating Rh-FF with added salt, [NaCl] = 4.79 mol L^{-1}, and (b) intensity profiles of the liposome shown in part a.

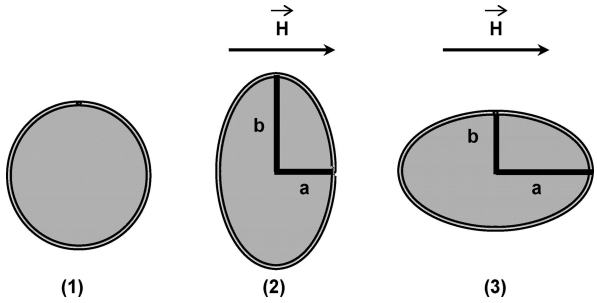

Figure 8. Deformation of a spherical magnetoliposome (1) into either an oblate ellipsoid (2) or a prolate ellipsoid (3) in an applied magnetic field.

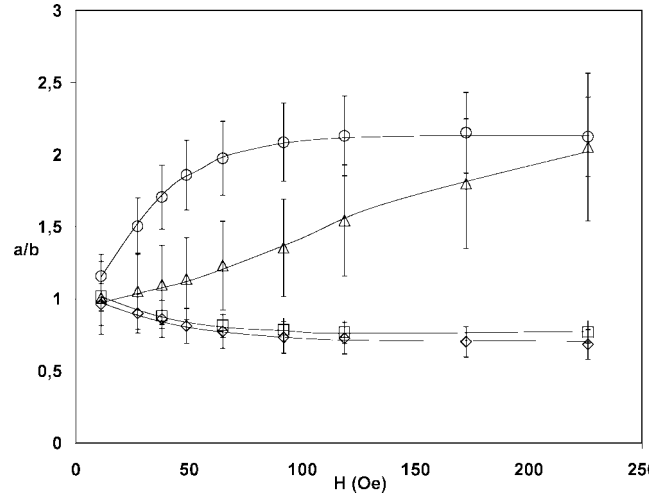

Figure 9. Experimental curves of the deformation of liposomes filled with fluorescent Rh-FF, where □ denotes [NaCl] = 0 mol L^{-1} (mean of 8 liposomes) and ○ denotes [NaCl] = 2.74 mol L^{-1} (mean of 9 liposomes). For liposomes filled with Cit-FF, ◇ denotes [NaCl] = 0 mol L^{-1} (mean of 8 liposomes) and △ denotes [NaCl] = 2.74 mol L^{-1} (mean of 14 liposomes).

the image is fully dark, which explains why no fluorescence was visualized inside the liposomes. At a high salt concentration, even when the fluorescence seemed homogeneously distributed over the volume (Figure 6b), the fluorescence plot profiles showed that the fluorescence was reinforced near the membrane (Figure 7).

Effect of Salt on the Elastic Properties of the Bilayer. Spherical magnetic liposomes elongate into oblate or prolate ellipsoids in an applied magnetic field. The overall shape depends on the ionic strength of the initial magnetic fluid.[4] Deformations are oblate ($a/b < 1$) at low ionic strength and prolate ($a/b > 1$) at high ionic strength (Figure 8).

Figure 9 shows a comparison of the deformation of Rh-FF liposomes and Cit-FF liposomes with and without NaCl ([NaCl] = 2.74 mol L^{-1}). For both liposomes, the deformation is mainly oblate without NaCl and prolate at higher ionic strength, in accordance with previously reported studies on magnetoliposomes with encapsulated citrate-coated particles.[4]

The deformation of quasi-spherical magnetoliposomes into prolate ellipsoids in an applied magnetic field can be explained by the flattening of thermal undulations due to the magnetic stress. The prolate ellipsoid obtained is defined by the eccentricity, e, where $e = [1 - (b/a)^2]^{1/2}$, a is the semiaxis of the liposome parallel to the magnetic field, and b is the value of the two other semiaxes orientated perpendicular to the magnetic field.

The basics of the model describing the deformation of isolated magnetic liposomes have been established previously in the case of a weak magnetic field,[22] and were later extended to the case of ellipsoids of any elongation.[23] The eccentricity of the liposomes is linked to the applied magnetic field through the following expression

$$\frac{16\pi K_b}{kT}(f(e)-1)+\ln\left(\frac{8\pi K_b}{45kT}g(e)^2\right)=4\ln\left(\frac{H}{H^*}\right) \quad (5)$$

where K_b is the bending modulus and H^* is a reduced parameter homogeneous to the magnetic field

$$H^{*2}=\sqrt{\frac{45kT}{32\pi K_b}}\frac{4}{\mu_0(\mu-1)^2}\frac{\tau_0}{R^0_{ves}} \quad (6)$$

where $f(e)$ and $g(e)$ are functions of eccentricity

$$f(e)=\left(\sqrt{1-e^2}+\frac{\arcsin(e)}{e}\right)\frac{1}{2(1-e^2)^{1/6}} \quad (7)$$

$$g(e)=\left(\frac{\frac{3-2e^2}{e^2}-(3-4e^2)\frac{\arcsin(e)}{e^3(1-e^2)^{1/2}}}{(1-e^2)^{2/3}\left(\left(\frac{3-e^2}{e^5}\right)\ln\left(\frac{1+e}{1-e}\right)-\frac{6}{e^4}\right)}\right) \quad (8)$$

Figure 11 shows a plot of eq 5 as solid lines in a semilog plot for $K_b = 20$ kT.

When using optical microscopy, we noticed that the prolate deformation of the Cit-FF and Rh-FF liposomes was greater with added salt ($e = 0.80$) compared with the elongation obtained with conventional liposomes ($e = 0.55$) under the same magnetic field (Figure 10).

This significant example also indicates that the liposome deformation does not continue to increase above [NaCl] = 2.74 mol L^{-1}. An interesting observation was the greater elongation under the magnetic field of liposomes encapsulating Rh-FF with a high salt concentration, even though their membranes did not exhibit thermal fluctuations (Figure 3). Figure 11 shows a comparison between liposomes filled with citrate-coated particles and liposomes filled with rhodamine-modified particles. The eccentricity of the prolate ellipsoid was measured as a function of the magnetic field intensity and plotted as e^4 versus ln(H/H^*).[2] The experimental curves were constructed for several liposomes (5 liposomes for [NaCl] = 0 mol L^{-1}, 12 liposomes for [NaCl] = 2.74 mol L^{-1}, and 7 liposomes for [NaCl] = 4.79 mol L^{-1}). The black symbols denote a comparison of the deformation of conventional magnetoliposomes. The experimental points fit the theoretical curve calculated using $K_b = 20$ kT.[23]

The experimental values of e^4 are much higher in the case of magnetoliposomes prepared with added salt (2.74 or 4.79 mol L^{-1}), while the deformation of liposomes encapsulating Rh-FF and Cit-FF were similar. The value of the bending modulus was determined only for the sample without added salt because this sample corresponds to the entropic behavior of the bilayer described by Helfrich.[24] In the presence of salt, the deformation starts from a spherical liposome, which exhibits no thermal fluctuations, and so this theory cannot be applied. However, we noticed that when the salt concentration increased ([NaCl] = 2.74 or 4.79 mol L^{-1}), the maximum eccentricity was much more important, $e^4 \approx 0.5$ compared to $e^4 \approx 0.15$. In addition, the gradient of the first part of the curve increased markedly, which is consistent with the important deformations observed previously.

Thus, if the deformations are related to the magnetophoresis experiments, then the important deformations and the high encapsulation rate are not influenced by rhodamine B but only by the ionic strength. On the other hand, for Cit-FF-based liposomes, we did not find the nonfluctuating membrane noticed previously for [NaCl] = 4.79 mol L^{-1}. It appears that the nanoparticles coated with rhodamine B interact with the membrane, which causes the thermal fluctuations to disappear.

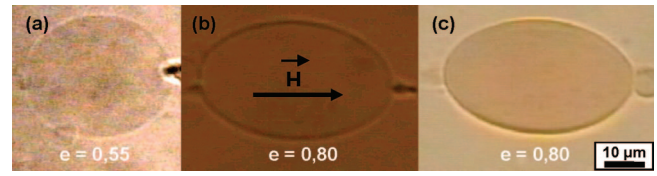

Figure 10. Optical microscopic images of Rh-FF-L under the same magnetic field, $H = 226$ Oe: (a) [NaCl] = 0 mol L^{-1}; (b) [NaCl] = 2.74 mol L^{-1}; (c) [NaCl] = 4.79 mol L^{-1}.

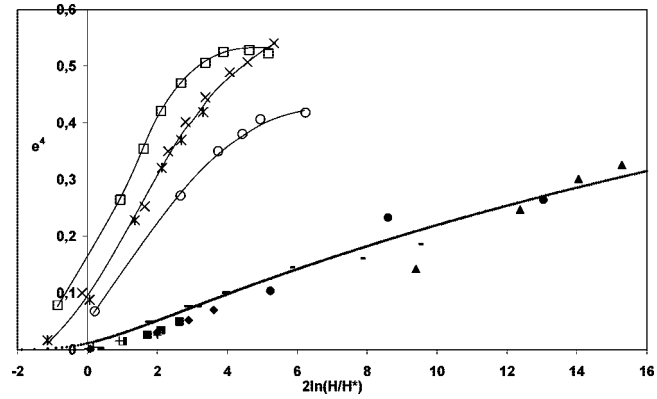

Figure 11. The symbols denote the experimental values of e^4 at different salt concentrations versus the natural logarithm of the square of the reduced magnetic field, ln(H/H^*). For liposomes filled with Rh-FF, ○ denotes [NaCl] = 2.74 mol L^{-1} (mean of 12 liposomes) and ∗ denotes [NaCl] = 4.79 mol L^{-1} (mean of 7 liposomes). For liposomes filled with Cit-FF, □ denotes [NaCl] = 2.74 mol L^{-1} (mean of 8 liposomes) and × denotes [NaCl] = 4.79 mol L^{-1} (mean of 13 liposomes). The deformations of conventional liposomes were fitted by the theoretical curve calculated using $K_b = 20$ kT. In this case, the different black symbols refer to the deformation of several liposomes.

Discussion

High Susceptibility Values. The important magnetic susceptibilities obtained for magnetic and fluorescent liposomes, which were up to 100 times higher than the values of conventional liposomes, have two causes. First, we know that a high ionic strength of the magnetic fluid increases its encapsulation rate inside the liposome. However, another phenomenon occurs at the highest ionic strength. The second cause is that the screening of electrostatic interparticle repulsions causes the aggregation of particles, and this aggregation appears before the flocculation in the phase diagram of the magnetic fluid in the presence of salt.[25] The magnetic susceptibility, χ, is proportional to nv^2, where n is the total number of aggregates and v is the mean volume of the aggregates. For example, an aggregation of 100 particles per group corresponds to a 100-times increase in volume, and in this case, n is divided by 100, so the magnetic susceptibility is 100 times higher.

Rhodamine−Membrane Interaction. The results of the epifluorescence measurements and the confocal microscopy showed a more intense fluorescence occurring at the membrane. This interaction can result from the presence of free rhodamine, as described in the literature. This property is used to target cells and organelle membranes with rhodamine B.[26] Under our experimental conditions (pH 7), the DOPC membrane bears a weak negative charge[27] and the rhodamine molecules have a positive charge. This increased fluorescence at the membrane may also arise from an interaction with the rhodamine grafted

to the particles. We demonstrated that the liposome membrane does not fluctuate when the initial magnetic fluid is a rhodamine B magnetic fluid, and when a large concentration of salt is added. In this case, the liposome membrane is unfolded completely and there is no thermal fluctuation. This unfolded membrane may result from an increase in the initial membrane tension caused by a particle−membrane interaction.

In the absence of an applied magnetic field, the membrane of a liposome in the fluidlike state fluctuates because of the thermal energy. When a magnetic field is applied, the membrane of the liposome unfolds completely until an ellipsoidal shape is obtained (Figure 8). The deformations observed here are classical and well suited to our model: oblate at weak ionic strength and prolate at high ionic strength. However, the eccentricity obtained when salt is added is much more important than that obtained at conventional ionic strength. This strong elongation is observed for Cit-FF and Rh-FF, indicating that this is not an effect of the rhodamine. This decrease in the bending rigidity may be discussed in terms of the effect of salt, as described in the literature in the case of a charged membrane.[28] In our study, the membrane and the particles were negatively charged, and the screening of the electrostatic repulsion between the membrane and the particles probably led to an interaction between the magnetic particles and the membrane.

From a physical point of view, this strong elongation cannot be explained by the unfolding of the thermal fluctuations. The deformation in the classical model is caused by two components: the previously explained membrane unfolding and the elastic deformation of the liposome corresponding to the stretching of the membrane. In the case of magnetoliposomes filled with a salty magnetic fluid, surface calculations highlight the fact that the surface area of the membrane increases when a magnetic force is applied. When the magnetic field is removed, the surface area is the same as the initial area, demonstrating an elastic behavior. The most interesting point is that this new elastic behavior shows, for the first time, a case of magnetoliposome deformation and a new model for this elastic elongation under a magnetic field.

Conclusions

The effect of salt allows one to obtain highly magnetic liposomes, and rhodamine-grafted magnetic nanoparticles allow us to enhance the fluorescent properties. The rhodamine−nanoparticle coupling changes the physicochemical properties of the membrane, weakening first the thermal fluctuations, leading to a marked increase in membrane stretching. This important elastic property will be studied in detail in another paper because in this case we cannot use a bending model alone but must involve a dual bending−stretching model. The deformation curves of liposomes demonstrated that, despite the nonfluctuating membrane, increasing the concentration of salt in the rhodamine magnetic fluid still induces an important elongation, which can be linked to recent data on the effect of salt in charged membranes. The surface calculations showed that the liposome volume is not constant and the membrane becomes stretched. Two factors, the high magnetic susceptibility and the interactions of the rhodamine-grafted particles with the membrane, allow one to access this new stretching regime under a magnetic force.[29,30] This stretching mode has been obtained in the case of a suction micropipette process.[29] For biomedical applications, the size of this type of liposome could be decreased by extrusion to obtain LUV, which could be used as contrast agents for MRI and fluorescence microscopy.

Acknowledgment. The authors thank Aude Michel for chemical synthesis, Delphine Talbot for chemical analysis, and Andrejs Cebers for helpful discussions.

Supporting Information Available: Table showing the magnetic susceptibilities of vesicles. This material is available free of charge via the Internet at http://pubs.acs.org.

References and Notes

(1) Park, S. H.; Oh, S. G.; Mun, J. Y.; Han, S. S. *Colloids Surf., B* **2006**, *48*, 112–118.
(2) Kloepfer, J. A.; Cohen, N.; Nadeau, J. L. *J. Phys. Chem. B* **2004**, *108*, 17042–17049.
(3) Wijaya, A.; Hamad-Schifferly, K. *Langmuir* **2007**, *23*, 9546–9550.
(4) Sandre, O.; Ménager, C.; Prost, J.; Cabuil, V.; Bacri, J. C.; Cebers, A. *Phys. Rev. E* **2000**, *62*, 3865–3870.
(5) Lesieur, S.; Grabielle-Madelmont, C.; Menager, C.; Cabuil, V.; Dadhi, D.; Pierrot, P.; Edwards, K. *J. Am. Chem. Soc.* **2003**, *125*, 5266–5267.
(6) Hamada, T.; Miura, Y.; Ishii, K.-I.; Araki, S.; Yoshikawa, K.; Vestergaard, M.; Takagi, M. *J. Phys. Chem. B* **2007**, *111*, 10853–10857.
(7) Babincova, M.; Leszczynska, D.; Sourivong, P.; Babinec, P. *Cell. Mol. Biol. Lett.* **1999**, *4*, 625–630.
(8) Bulte, J. W. M.; De Cuyper, M.; Despres, D.; Frank, J. A. *J. Magn. Magn. Mater.* **1999**, *194*, 204–209.
(9) Martina, M.-S.; Fortin, J.-P.; Ménager, C.; Clément, O.; Barratt, G.; Grabielle-Madelmont, C.; Gazeau, F.; Cabuil, V.; Lesieur, S. *J. Am. Chem. Soc.* **2005**, *127*, 10676–10685.
(10) Kawai, N.; Ito, A.; Nakahara, Y.; Honda, H.; Kobayashi, T.; Futakuchi, M.; Shirai, T.; Tozawa, K.; Kohri, K. *Prostate* **2006**, *66*, 718–727.
(11) Toyota, T.; Tsuha, H.; Yamada, K.; Takakura, K.; Yasuda, K.; Sugawara, T. *Langmuir* **2006**, *22*, 1976–1981.
(12) Gopalakrishnan, G.; Danelon, C.; Izewska, P.; Prummer, M.; Bolinger, P.-Y.; Geissbühler, I.; Demurtas, D.; Dubochet, J.; Vogel, H. *Angew. Chem., Int. Ed.* **2006**, *45*, 5478–5483.
(13) Baumgart, J.; Hess, S. T.; Webb, W. W. *Nature* **2003**, *425*, 821–824.
(14) Tamba, Y.; Yamazaki, M. *Biochemistry* **2005**, *44*, 15823–15833.
(15) Inaoka, Y.; Yamazaki, M. *Langmuir* **2007**, *23*, 720–728.
(16) Scheffold, A.; Miltenyi, S.; Radbruch, A. *Immunotechnology* **1995**, *1*, 127–137.
(17) Martina, M.-S.; Fortin, J.-P.; Fournier, L.; Ménager, C.; Gazeau, F.; Clément, O.; Lesieur, S. *Mol. Imaging* **2007**, *6*, 140–146.
(18) Beaune, G.; Dubertret, B.; Clément, O.; Vayssettes, C.; Cabuil, V.; Ménager, C. *Angew. Chem., Int. Ed.* **2007**, *46*, 5421–5424.
(19) Bertorelle, F.; Wilhelm, C.; Roger, J.; Gazeau, F.; Ménager, C.; Cabuil, V. *Langmuir* **2006**, *22*, 5385–5391.
(20) Massart, R. *IEEE Trans. Magn.* **1981**, *17*, 131.
(21) Foner, S. *Rev. Sci. Instrum.* **1959**, *30*, 548–557.
(22) Bacri, J.-C.; Cabuil, V.; Cebers, A.; Menager, C.; Perzynski, R. *Europhys. Lett.* **1996**, *33*, 235–240.
(23) Ménager, C.; Meyer, M.; Cabuil, V.; Cebers, A.; Bacri, J.-C.; Perzynski, R. *Eur. Phys. J. E* **2002**, *7*, 325–337.
(24) Helfrich, W. *Naturforsch* **1973**, *28c*, 693–694.
(25) Dubois, E.; Cabuil, V.; Boué, F.; Bacri, J. C.; Perzynski, R. *Prog. Colloid Polym. Sci.* **1997**, *104*, 173–176.
(26) Reungpatthanaphong, P.; Dechsupa, S.; Meesungnoen, J.; Loetchutinat, C.; Mankhetkorn, S. *J. Biochem. Biophys. Methods* **2003**, *57*, 1–16.
(27) Quemeneur, F.; Rammal, A.; Rinaudo, M.; Pépin-Donat, Brigitte. *Biomacromolecules* **2007**, *8*, 2512–2519.
(28) Delorme, N.; Bardeau, J.-F.; Carrière, D.; Dubois, M.; Gourbil, A.; Mohwald, H.; Zemb, Th.; Fery, A. *J. Phys. Chem. B* **2007**, *111*, 2503–2505.
(29) Evans, E.; Rawicz, W. *Phys. Rev. Lett.* **1990**, *64*, 2094–2097.
(30) Kwok, R.; Evans, E. *Biophys. J.* **1981**, *35*, 637–652.

JP711811U